Supplementary Information

Article Title: SNO–Hemoglobin Not Essential for Red Blood Cell Dependent Hypoxic Vasodilation

Authors: T. Scott Isbell[1,#], Chiao–Wang Sun[2,#], Li–Cheyn Wu[2], Xinjun Teng[1], Dario A. Vitturi[1], Billy G Branch[3], Christopher G Kevil[3], Ning Peng[4], JM Wyss[4], Namasivayam Ambalavanan[4,5] Lisa Schwiebert[6], Jinxiang Ren[2], Kevin M. Pawlik[2], Matthew B. Renfrow[2], Rakesh P. Patel[1,*], Tim M. Townes[2]

Methods

Production of knockin mice

The replacement of mouse alpha- and beta-globin genes with human alpha- and beta-globin genes was performed essentially as described[1]. Specific methods are described in supplemental Fig 2, panels a-c.

Red Blood Cell Thiol Measurements

RBC glutathione was measured by addition of 400uL 5% TCA to 100 uL RBCs followed by centrifugation (14,000 g, 3 min, 4°C) to precipitate proteins. Supernatant is then diluted 1:10 in PBS + 10uM DTPA + 0.1% Triton X and GSH measured as previously described[2]. Hemoglobin total and surface accessible reduced thiol were measured as previously described[3]. Whole blood was collected via cardiac puncture into 1 mL syringes containing 100µl of acid citrate dextrose as an anti-coagulant. Whole blood was then centrifuged for 90 seconds at 22^{o}C and the plasma and buffy coat were removed. The RBC pellet was washed two times with PBS and then lysed hypotonically with cold distilled water. Lysates were incubated with 5,5'-dithiobis-(2-nitrobenzoic acid) (DTNB) to measure free sulfhydryl groups present in proteins and peptides. The resulting 2-nitro-

thiobenzoic acid (TNB) formed was measured spectrophotometrically at 412 nm and concentration calculated with the molar extinction coefficient (ε = 14,150 M-1 cm-1). To determine the contribution of hemoglobin thiols, lysates were passed down a G25 sepharose column and the hemoglobin fraction (MW >10 kDa) collected and incubated with DTNB in the absence or presence of 0.1% (v/v) SDS to access surface versus total thiol content, respectively.

Hematology

Blood was collected from anesthetized animals into Microtainer EDTA collection tubes (Becton Dickinson). The following hematological parameters: RBC count (10^6/μl) , hemoglobin concentration (g/dL), mean corpuscular volume (MCV, fL) and mean corpuscular hemoglobin (MCH, pg) were measured on a HemaVet 1700 (CDC Technology, Oxford, CT) hematology analyzer. Packed cell volume (PCV) was measured with a JorVet J503 (Jorgenson Laboratories Systems, Loveland, CO) microhematocrit centrifuge. Reticulocyte counts were determined by flow cytometry after staining with thiazole orange.

Hemoglobin Oxygen Affinity

Visible spectra of intra-erythrocytic hemoglobin were obtained with a Cary 14 (AVIV Associates) equipped with a scattered transmission accessory and a polarographic O_2 sensor (2110; Orbisphere) as described previously [4]. Briefly, erythrocyte suspensions at 0.3% hematocrit in PBS were equilibrated in a sealed quartz cuvette under a stream of humidified air for 10 minutes at 37°C with constant stirring before switching to 100% nitrogen. Spectral changes between 535 and 585 nm and the oxygen tension in the

cuvette were recorded until deoxygenation was complete. Half-fractional saturation values were obtained by adjusting data to the following equation: $Y = O_2^n/O_2^n+P_{50}^n$ using the Levenberg-Marquardt algorithm included in Microcal Origin 6.1 where Y = fractional saturation, O_2=Oxygen tension in mm Hg, P50 = Half fractional saturation and n = Hill number.

Hemodynamics

Hemodynamic parameters were measured either non-invasively using a specialized differential pressure transducer tail cuff (Kent Scientific). Male mice (8 weeks of age) were first acclimated to the blood pressure measuring apparatus following manufacturer recommendations to obtain steady baseline values. Upon reaching stable baseline readings blood pressure was recorded over three days and mean values calculated for each animal. Alternatively, MAP was determined using arterial catheters as described in supplemental Fig 4.

Right ventricular pressure, a direct correlate of pulmonary pressure, was measured directly by insertion of a 23G needle into the right ventricle after anesthesia and thoracotomy. In the same set of animals the chronic effects of pulmonary hypertension were assessed on formalin fixed hearts by the Fulton Index (right ventricle weight/ [left ventricle weight + septum weight]). In addition H&E stained sections of lung were assessed for vascular remodeling (increased wall thickness) secondary to pulmonary hypertension.

Vessel Bioassays

For all vessel experiments pulmonary arteries from female New Zealand White rabbits (2.5 kg) were used. Briefly, pulmonary arteries were isolated and submerged in Krebs-Henseleit (KH) buffer maintained at room temperature. Vessels were cleansed of fat and connective tissue and segmented into 2-3 mm rings. Vessel rings were then mounted in vessels bioassay chambers (Radnoti Glass Technologies) containing 15 ml of KH buffer and perfused with a gas mixture comprising 21% O_2/ 5% CO_2/ 74% N_2 at 37^{o}C, pH 7.45. A basal tension of 1 g was applied and vessel rings allowed to equilibrate for 1 hr. Following equilibration a hyperpolarizing dose of KCl (70mM) was added to the baths to check for viability and assess maximum constriction.

To measure hypoxic vasodilation by HbC93 or HbC93A RBC, vessels were equilibrated at a 0% O_2 gas mixture (containing 5% CO_2 and balanced with N_2). Gas was precisely delivered by mass flow controllers (Sierra Instruments, California, USA) set to 0.15L/min. In all runs vessels were pretreated with indomethacin (5 μM) to block cyclooxygenase. Vessels were pre-constricted to approximately 50-75% of maximal KCl tension with L-phenylephrine (PE, 100 nM). Whole blood from either HbC93 of HbC93A mice was collected as described above and the RBC pellet washed once with PBS. A 0.3% final Hct of either control or mutant RBC was then immediately added to the baths. Vasodilatory effects were determined by measuring the change in tension and expressing this as a percent relaxation with respect to the maximal PE constriction. Vessel bioassay experiments were performed in decreased lighting to protect photo-labile RSNO.

Measurement of Nitric Oxide Metabolites

For the measurement of blood nitric oxide metabolites, blood was collected via cardiac puncture into 1mL syringes containing 1.5% (w/v) sodium citrate, 5 mM NEM, and 100 μM DTPA (all concentrations listed are final). After mixing, blood was centrifuged at 2000 x g for 90 seconds at 25^{o}C and plasma removed and further stabilized with 1 mM NEM and 100 μM DTPA. For the determination of RBC RSNO and XNO, the red blood fraction was stabilized in a solution containing 10mM potassium ferricyanide, 20 mM NEM, 1% (v/v) NP-40 and 100 μM DTPA in PBS. For the determination of whole blood levels of nitrite, samples were collected as above and then stabilized with 0.13M potassium ferricyanide, 1.67 mM NEM and 1% NP40 (v/v). Prior to analysis samples for whole blood nitrite determination were de-proteinized with a equal volume addition of 100% methanol and then centrifuged at 14 000 x g for 5 min. Total NO metabolites (nitrite, RSNO and XNO) were measured by a reductive (I_3^-) chemiluminescence method as previously described[5]. To specifically determine the individual components samples were pre-treated with either acid sulfanilamide or acid sulfanilamide + Hg to selectively remove nitrite and RSNO, respectively. Quantitation was performed by comparison to a nitrite standard curve. For RBC measurements, samples were also passed through Sephadex G-25 gel-filtration column (pre-equilibrated with PBS + 10μM DTPA) to assess S-nitrosothiol distribution between high Mwt (>10KDa, hemoglobin containing) and low Mwt (<10 kDa) fractions.

Exercise Stress Tests

Graded treadmill exercise tests were performed (Exer6M) using male mice. Mice were allowed to warm up for 5 min at 10m/min and then speed was increased by 3 meters every 3 minutes to a maximum speed of 30m/min. During the endurance exercise test

male mice were allowed to warm up for 10 minutes at 10m/min and speed increased to 15m/min for 30 minutes. Thereafter speed was increased by 3 meters every 30 minutes to a final of 27m/min. In each case time to fatigue was recorded when mice could no longer maintain a running pace despite external stimuli.

LC-MS/MS of globin polypeptides

Hemolysates were prepared from HbC93 mice by lysis of RBC in water, and membranes were pelleted by centrifugation. The supernatant was adjusted to 2% SDS, 0.1 mM mercaptoethanol and globin polypeptides were separated by SDS-PAGE. Proteins were stained with coomassie, and globin polypeptides were excised with a razor blade. The excised proteins were subjected to in-gel tryptic digestion (with reduction by 10 mM dithiothreitol and alkylation with iodoacetamide). The tryptic digests were loaded onto a LC-MS system composed of a MicroAS autosampler, 2D LC nanopump (Eksigent, Dublin, CA), and a linear ion trap-Fourier transform ion cyclotron resonance hybrid mass spectrometer (LTQ FT, Thermo Scientific, San Jose, CA). The pulled tip was packed with Jupiter 5 μm C18 revered phase beads to give a 100 μm diameter, 11 cm column. A gradient of acetonitrile with 0.1% formic acid was run from 5-30% in 60 minutes at 500 nl min^{-1}. LTQ FT parameters were set as previously described[6]. Hb tryptic peptides were identified by use of the TurboSEQUEST algorithim within Bioworks 3.2 (Thermo Scientific) with a mass accuracy of 2.0 ppm or better. Independent LC-MS analysis of the HbC93 and HbC93A polypeptides revealed the presence of a unique tryptic fragment in each sample. For the HbC93 polypeptide, an ion species corresponding to the tryptic fragment ^{83}GTFATLSELHCDK^{95} was confirmed by both mass accuracy (theoretical

mass: 1477.6871 Da, observed mass: 1477.6848, mass error: -1.54 ppm) and tandem mass spectrometry (MS/MS, Figure 1 D). For the HbC93A polypeptide a distinct ion species corresponding to the tryptic fragment ^{83}GTFATLSELHADK^{95} was confirmed in similar fashion (theoretical mass: 1388.6936, observed mass: 1388.6924, mass error: -0.432 ppm, Figure 1 E). No trace of the native HbC93 tryptic peptide was observed in the HbC93A LC-MS analysis.

Capillary Density Determination

Transverse sections of the hearts from HbC93 and HbC93A mice were frozen in OCT compound (Sakura Finetek USA, Inc., Torrance, CA). 10μm frozen cross-sections were fixed with 95% ethanol/5% glacial acetic acid for 20 minutes at –20°C, washed three times with PBS, blocked with 5% horse serum/PBS, and then stained with anti-mouse PECAM-1 (CD31) antibody (BD PharMingen) diluted 1:200 in PBS/0.05% horse serum followed by Cy3-conjugated anti-rat antibody diluted 1:250 in PBS with 0.05% horse serum. Slides were then mounted with Vectashield mounting medium containing 4,6-diamidino-2-phenylindole (DAPI) nuclear counterstain (Vector Laboratories, Inc., Burlingame, CA). Digital images were taken at a magnification of x200 on a Nikon Eclipse TE2000-S epifluorescent scope (Melville, NY) using Texas Red and DAPI excitation/emission filters in conjunction with a Hamamatsu Orca-ER digital camera (Bridgewater, NJ). The total pixel density of PECAM-1 and DAPI staining was quantified for each image using Simple PCI software (C-Imaging Systems; Compix Inc., Sewickley, PA). All imaging settings for each respective fluorochrome were kept constant between specimens and the amount of PECAM-1 and DAPI pixel density

measured using the image processing and analysis feature of Simple PCI. Total PECAM-1 pixel density was divided by the total DAPI pixel density for each image to calculate a vascular density ratio.

Supplementary Table 1. Hematological and urine concentration values of HbC93 and HbC93A mice.

All animals were analyzed between 2-5 mo of age. Values represent the mean ± SEM with p-values shown calculated by unpaired t-test. Number of replicates are also indicated in table with each 'n' value corresponding to an individual mouse. Key: RBC = Red blood cell, Hb = hemoglobin, PCV = packed cell volume or hematocrit, Retics = reticulocytes, RDW = red cell distribution width, MCV = mean corpuscular volume, MCH = mean corpuscular hemoglobin. Hemoglobin levels, red cell distribution widths, mean corpuscular volumes and mean corpuscular hemoglobins are slightly higher in HbC93A compared to HbC93 animals; however, the values are within the normal range. Reticulocyte levels, which are the most sensitive measure of anemia in mice, are not different in HbC93A compared to HbC93 animals. This result and the absence of differences in RBC hypoxic vasodilation and basal MAP suggest that the minor differences in Hb, RDW, MCV and MCH have no significant effect on basal vascular function via changes in blood viscosity and shear stress[7]

Mice	RBC x 10^6/µL	Hb g/dL	PCV %	Retics %	RDW %	MCV fL	MCH pg	Urine Conc. mOsm
HbC93	11.0 ± 0.13	10.4 ± 0.15	41.4 ± 0.48	7.8 ± 0.42	21.4 ± 0.35	35.5 ± 0.33	9.3 ± 0.09	2812 ± 110
HbC93A	11.1 ± 0.11	11.4 ± 0.1	42.2 ± 1.4	8.0 ± 0.43	23.2 ± 0.25	37.7 ± 0.39	10.3 ± 0.1	2568 ± 66.9
P-value	0.61	<0.0001	0.61	0.68	<0.0001	<0.0001	<0.0001	0.06
'n' value	35	35	26-33	29-35	35	35	35	15-19

Supplementary Figures

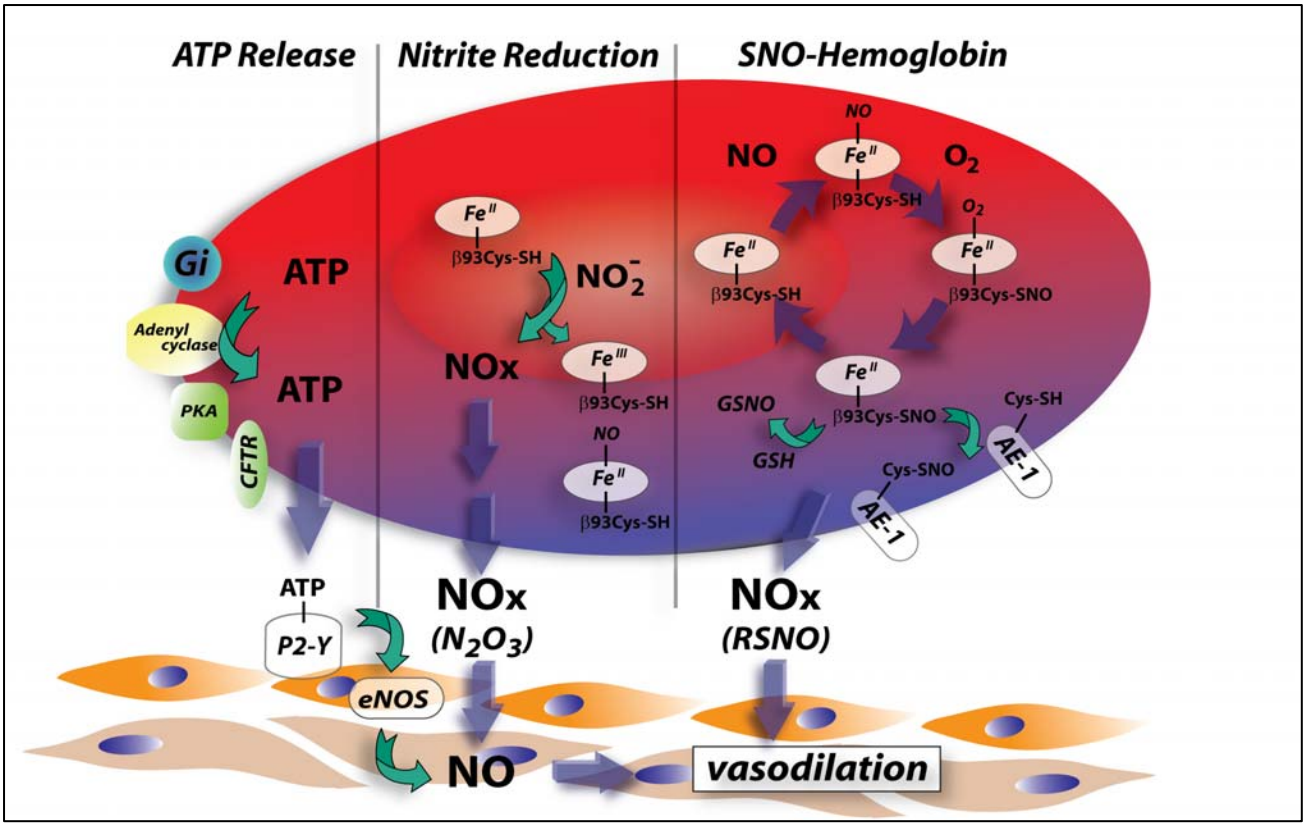

Supplementary Figure 1: Proposed mechanisms of RBC mediated hypoxic vasodilation

Proposed mechanisms for red blood cell (RBC) dependent hypoxic vasodilation follow the general paradigm of the coupling of hemoglobin deoxygenation to the activation of NO-dependent vasodilation in the vessel wall. Suppl Fig 1 illustrates the 3 proposed mechanisms that include ATP release, nitrite reduction to NO and S-nitrosohemoglobin (SNO-Hb) dependent bioactivity. *ATP release:* In the mid 1990's, Ellsworth and Sprague demonstrated that hypoxic RBC, but not normoxic RBC, release ATP[8,9]. This extracellular ATP binds to endothelial purinergic receptors (P_{2Y}), activates endothelial nitric oxide synthase and stimulates NO-dependent vasodilation[10,11]. Consistent with this mechanism, increased skeletal muscle blood flow in exercising humans is associated with increased plasma ATP[12] and more recent studies have provided insights into the signaling pathways in RBCs that mediate hypoxia dependent ATP release[13]. *Nitrite-reduction:* We

and others have suggested that nitrite reactions with deoxyhemoglobin are kinetically maximal around the hemoglobin P_{50}, resulting in methemoglobin (FeIII) and NO formation, the latter of which can nitrosylate ferrous hemoglobin forming nitrosylhemoglobin (FeII-NO) or stimulate vasodilation[4,14-16]. More recent studies have suggested that dinitrogen trioxide (N_2O_3) may be an intermediate in this reaction allowing NO-bioactivity to escape the RBC and mediate SNO-formation by this pathway (not shown)[17]. We note, the nitrite pathway is not the focus of the current study and we refer to recent studies and reviews discussing the pros- and cons of this pathway in more detail [4,14-28]. *SNO-Hb pathway:* In 1996[29], the Stamler laboratory and colleagues published the first in a series of seminal studies proposing that hemoglobin becomes S-nitros(yl)ated on a specific and conserved cysteine residue on the β-chain (β93Cys) as RBCs become oxygenated in the lungs (referred to herein in as SNO-Hb). In the R-state, SNO-Hb remains relatively unreactive but upon deoxygenation, T-state SNO-Hb can rapidly react with other key RBC thiols via transnitrosation reactions including GSH or thiols on the RBC membrane protein, anion exchanger-1 (AE-1). This in turn is proposed to transmit a vasodilatory signal out of the RBC[29-35]. However, several elements of this hypothesis have been challenged including i) oxygen sensitivity (and hence allosteric dependence) of SNO-Hb dependent vasodilation and transnitrosation reactions with other thiols[3,36-38], ii) in vivo SNO-Hb concentrations and presence of physiologic arterial-venous SNO-Hb gradients [39-41] and iii) mechanisms of SNO-Hb formation [42-45]. Finally we note that Suppl Fig 1 does not include other possible RBC-dependent mechanisms of blood flow control that may include the presence of the RBC endothelial nitric oxide synthase and modulation of vascular endothelial cell nitric oxide synthase activity by biophysical effects of the RBC hematocrit on blood viscosity and shear stress[7,46].

Supplementary Figure 2

2a

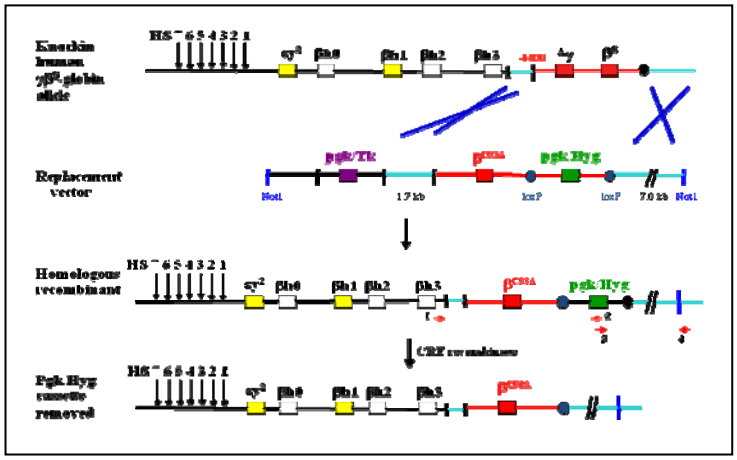

2b

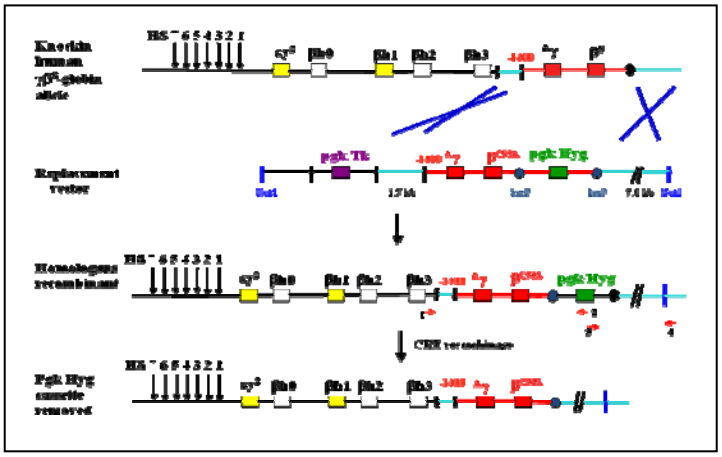

2c

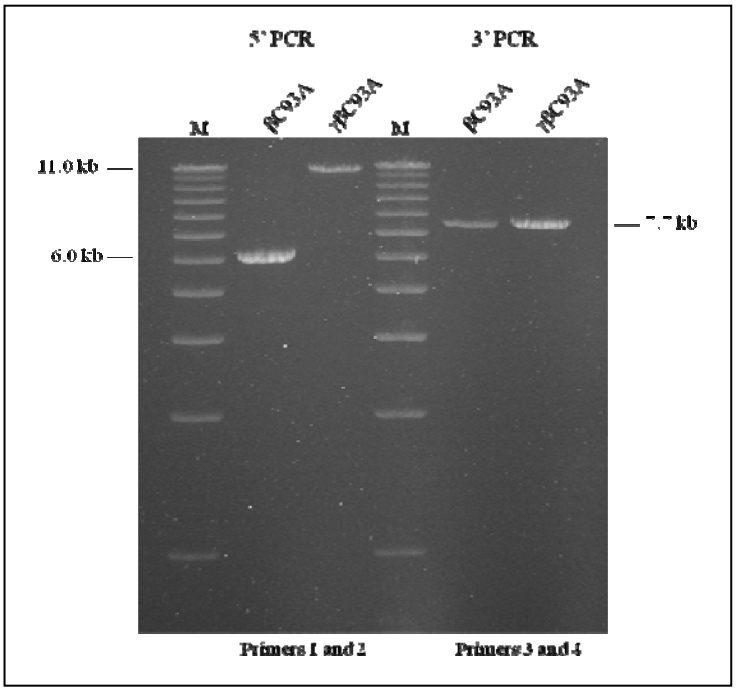

2d

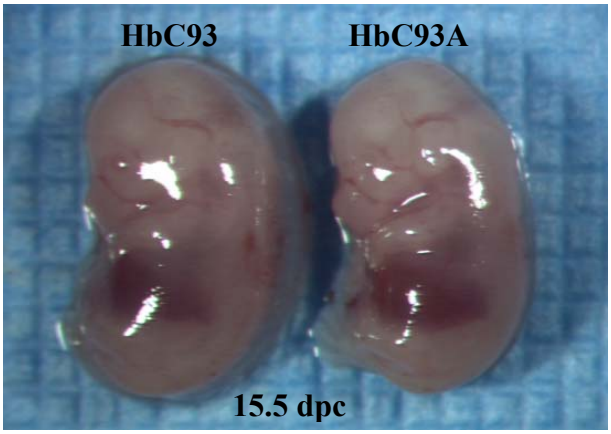

2e

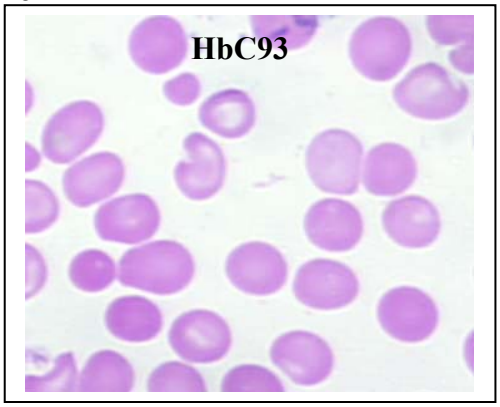

2f

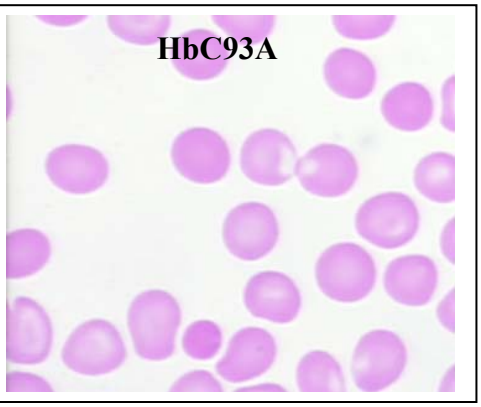

Supplementary Figure 2:

a. Schematic representation of gene replacement in knock-in sickle ES cells. The 20-kb replacement vector contains a 2.1-kb pgk/TK gene, 1.7 kb of mouse 5' flanking sequence, a -815 human βC93A-globin gene fragment (4.6 kb), a 1.8-kb floxed pgk/Hygro gene, and 7 kb of mouse 3' flanking sequence. Homologous recombinants were identified by PCR with primers 1 and 2 to identify correct 5' sequences (primer 1 is outside of the vector homology region) and with primers 3 and 4 to identify correct 3' sequences (primer 4 is outside of the vector homology region). **b.** Schematic representation of gene replacement in knock-in ES cells. The 25-kb replacement vector contains a 2.1-kb pgk/TK gene, 1.7 kb of mouse 5' flanking sequence, a -1400 βC93A fragment (9.7 kb), a 1.8-kb floxed pgk/Hygro gene, and 7 kb of mouse 3' flanking sequence. Homologous recombinants were identified by PCR with primers 1 and 2 to identify correct 5' sequences (primer 1 is outside of the vector homology region) and with primers 3 and 4 to identify correct 3' sequences (primer 4 is outside of the vector homology region). **c.** PCR analysis of two positive homologous recombinant ES cell lines. 5' PCR (primers 1 and 2) and 3' PCR (primers 3 and 4) from one βC93A knockin line and from one γβC93A knockin line are illustrated. Correct recombination at the 5' end is demonstrated by a 6.0 kb band for the βC93A knockin line. Correct recombination at the 3' end is demonstrated by a 7.7 kb band for both βC93A and γβC93A knockin lines. **d.** Homozygous βC93A and γβC93A knockin 15.5 dpc fetuses. No obvious differences in HbC93 and HbC93A fetuses were detected in vascularization, hemoglobinization of fetal liver or in total size of the fetus. **e** and **f.** Blood smears of HbC93 and HbC93A adult animals. Both HbC93 and HbC93A animals are slightly thalassemic (see suppl Table 1) since the human alpha-globin gene, which replaces mouse alpha-globin genes on chromosome 11, is expressed at a higher level than the human beta-globin gene, which replaces mouse beta-globin genes on chromosome 7. This minor over-expression of human alpha occurs when wild-type or mutated human beta-globin genes are utilized. Therefore, the minor alpha- to beta-globin chain imbalance is identical in control (HbC93) and betaC93A (HbC93A) animals. Note the same is true for our sickle globin gene knockin animals as described previously [1,47].

Supplementary Figure 3:

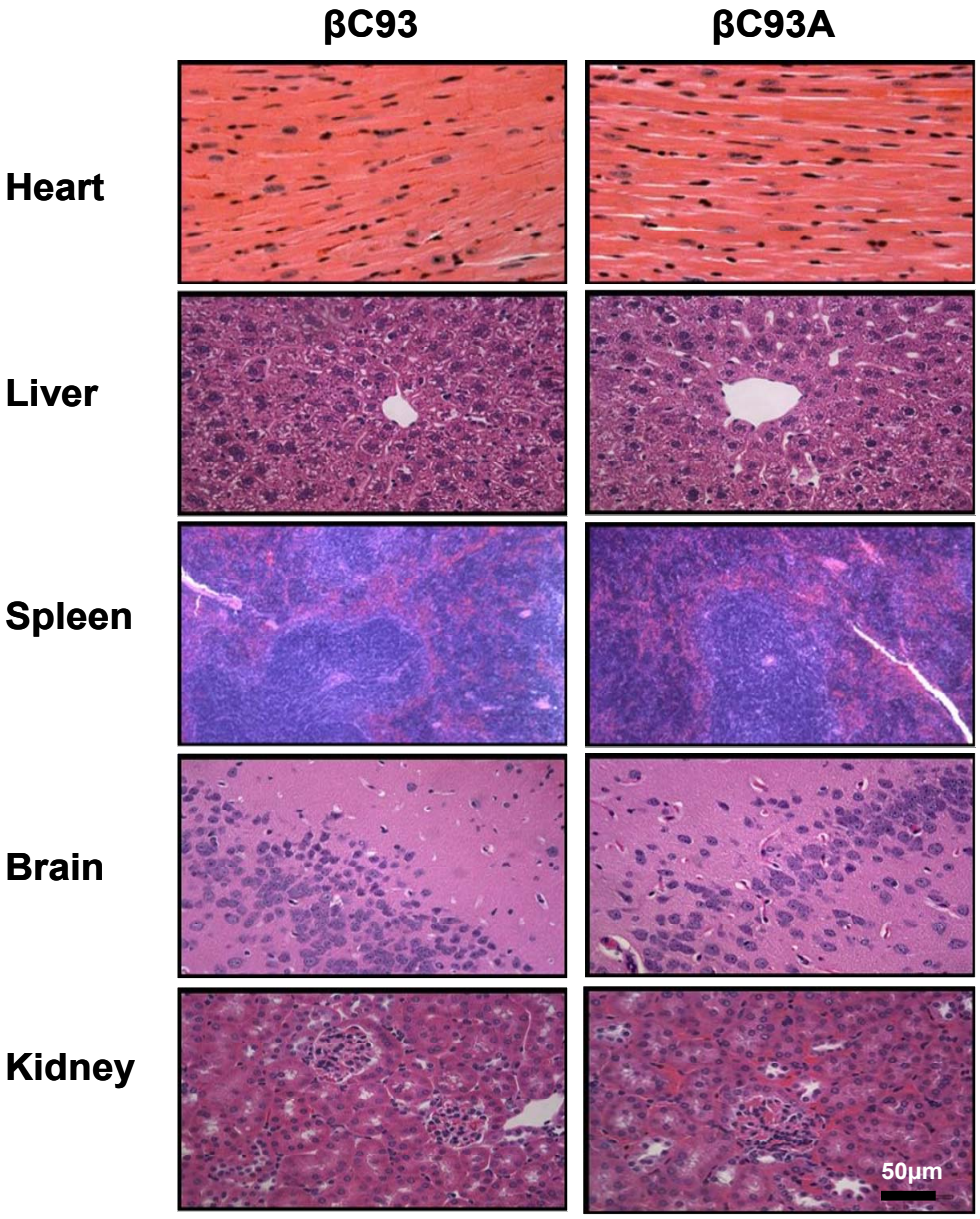

Supplementary Fig 3: **Representative micrographs of hematoxyln and eosin (H&E) stained tissues from HbC93 and HbC93A mice**. Tissues were fixed in 10% buffered formalin for 24 hrs. 5μm sections of each tissue were stained and visualized with 40x magnification. No notable histopathology was observed when assessed in a blinded manner.

Supplementary Figure 4:

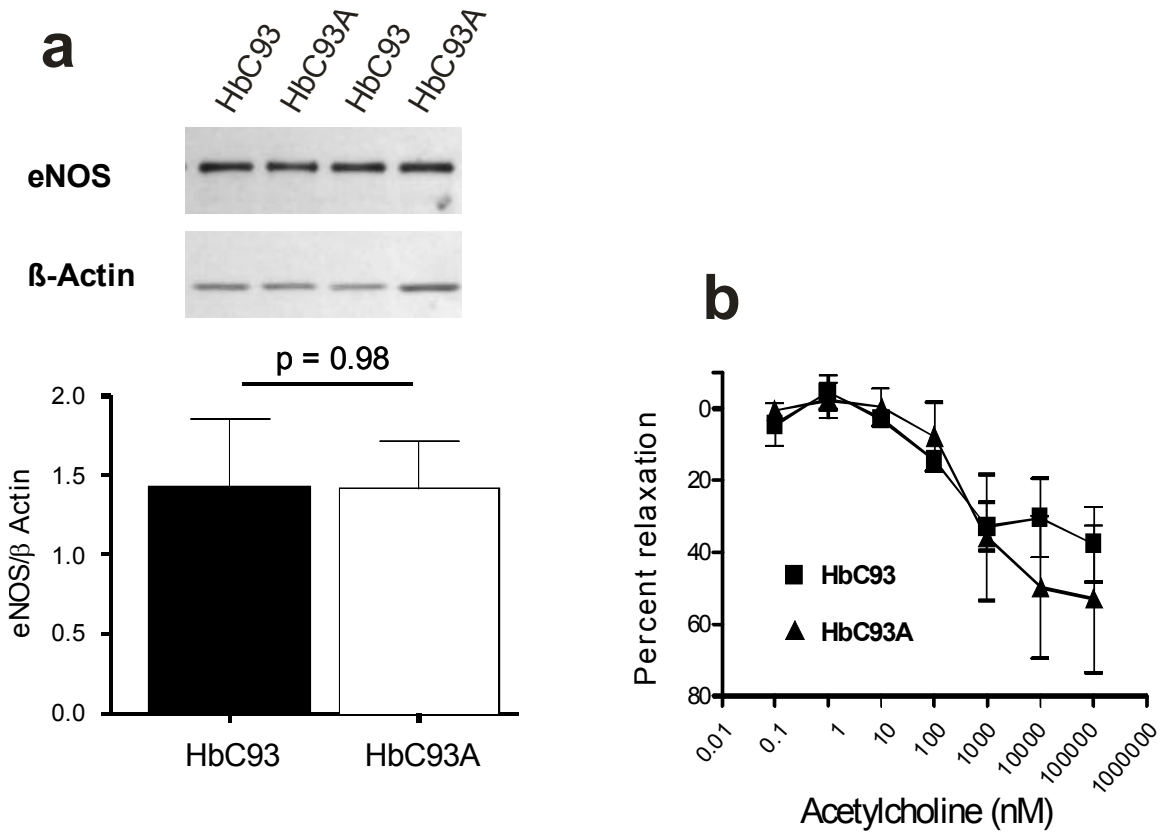

Supplementary Figure 4: eNOS expression and activity in HbC93 and HbC93A mice. a: eNOS expression was determined in aorta homogenates collected from HbC93 or HbC93A mice by Western blotting. Aortas were isolated from saline perfused mice, homogenized and clarified by centrifugation at 14 000 rpm for 5min at RT. Protein concentration of supernatant was determined by Lowry protein assay and 50 or 100ug protein was separated on a 10% reducing gel. Proteins were transferred to PVDF membranes and probed for total eNOS using a monoclonal antibody (BD Biosciences) and detected using an anti-mouse IgG secondary antibody conjugated to horse radish peroxidase in the presence of SuperSignal chemiluminescent substrate (Pierce, Illinois, USA). Additionally blots were stripped and probed for β-actin for normalization. Blots were quantitated by measuring band intensity using Alpha Innotech Software (California, USA) Shown are representative blots (from 2 mice each group) and bar graph showing mean ± SEM, n= 6. P-value determined by unpaired t-test. **b:** Acetylcholine mediated

vasodilation of aorta collected from HbC93 or HbC93A mice was determined as described in methods. Values show mean ± SEM, (n=3 mice per group). No significant difference between HbC93 and HbC93A mice was observed by 2-way ANOVA analysis (P= 0.75).

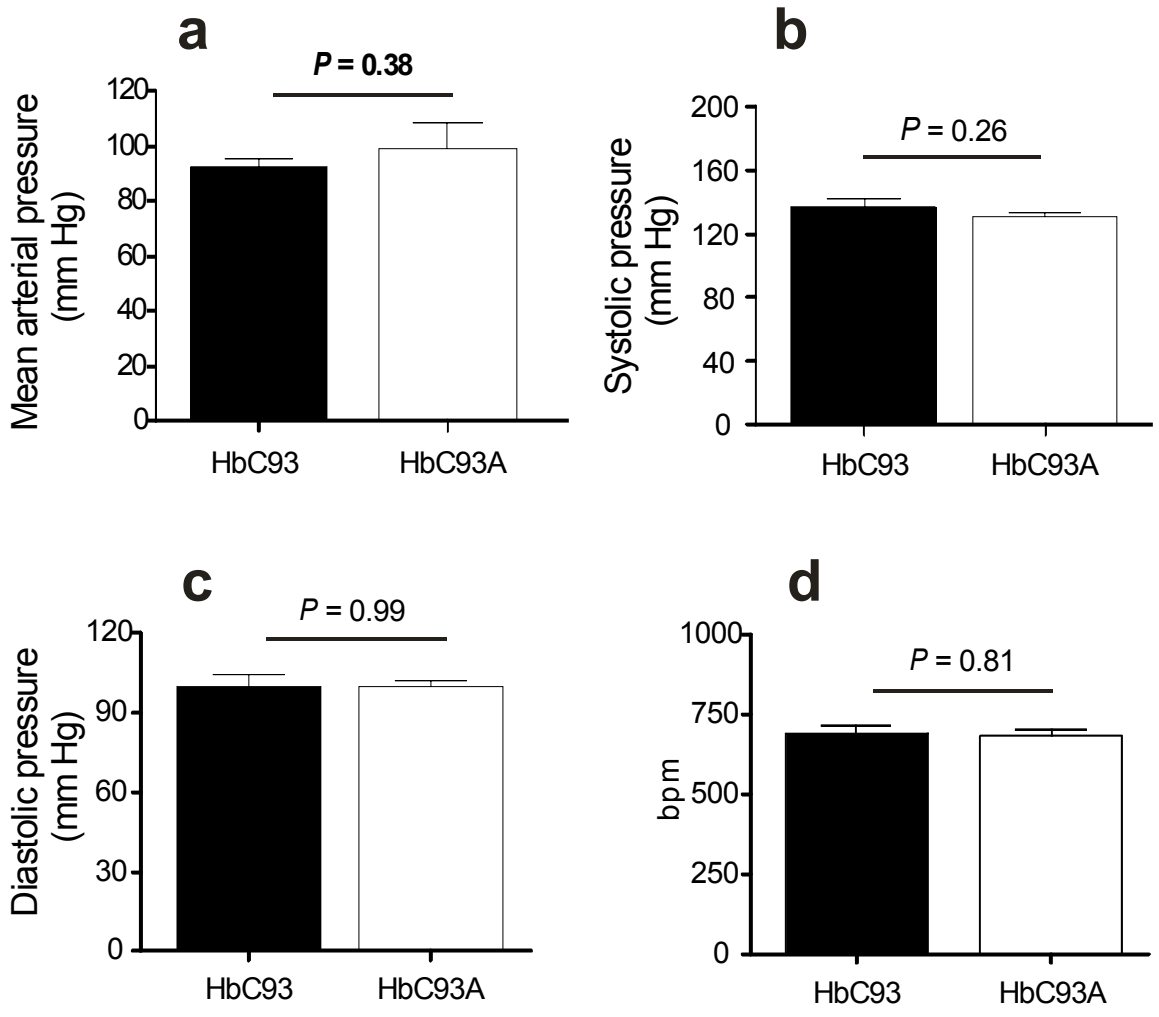

Supplementary Figure 5: a) mice were anesthetized with isoflurane and an arterial catheter was inserted into the carotid artery. Following closure of the wound the animal was recovered overnight prior to recoding of arterial pressure[48]. Arterial pressure recordings were made using a BioPac system[49]. Panels **b**–**d** show systolic blood pressure, diastolic blood pressure and heart rate respectively in conscious HbC93 and HbC93A mice as measured by tail-cuff using CODA-2 (see methods). No significant differences in these hemodynamic parameters were observed between HbC93 and HbC93A mice, P-values shown calculated by unpaired t-test. Data are mean ± SEM, n= 3-11

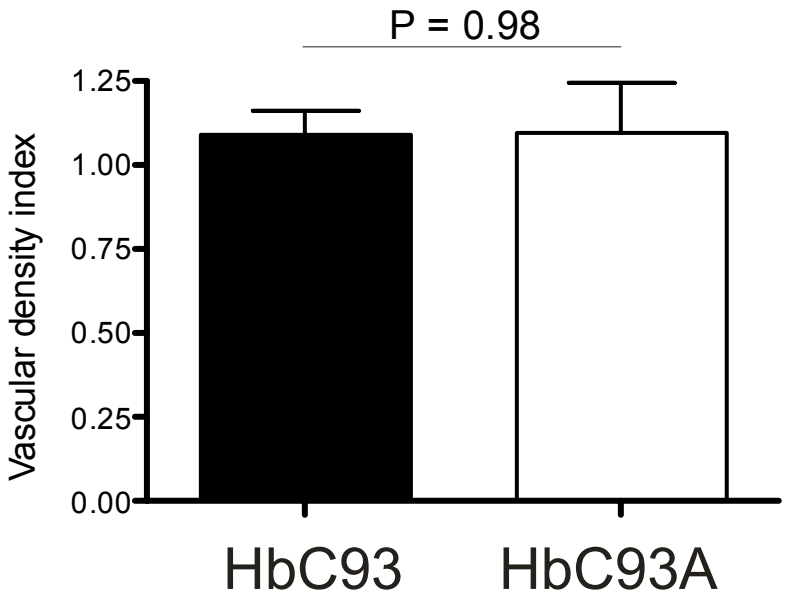

Supplementary Figure 6: Vascular density was evaluated in the heart as described in methods. No difference between HbC93 and HbC93A mice was observed. P-value calculated by unpaired t-test. Data show mean ± SEM (n=3).

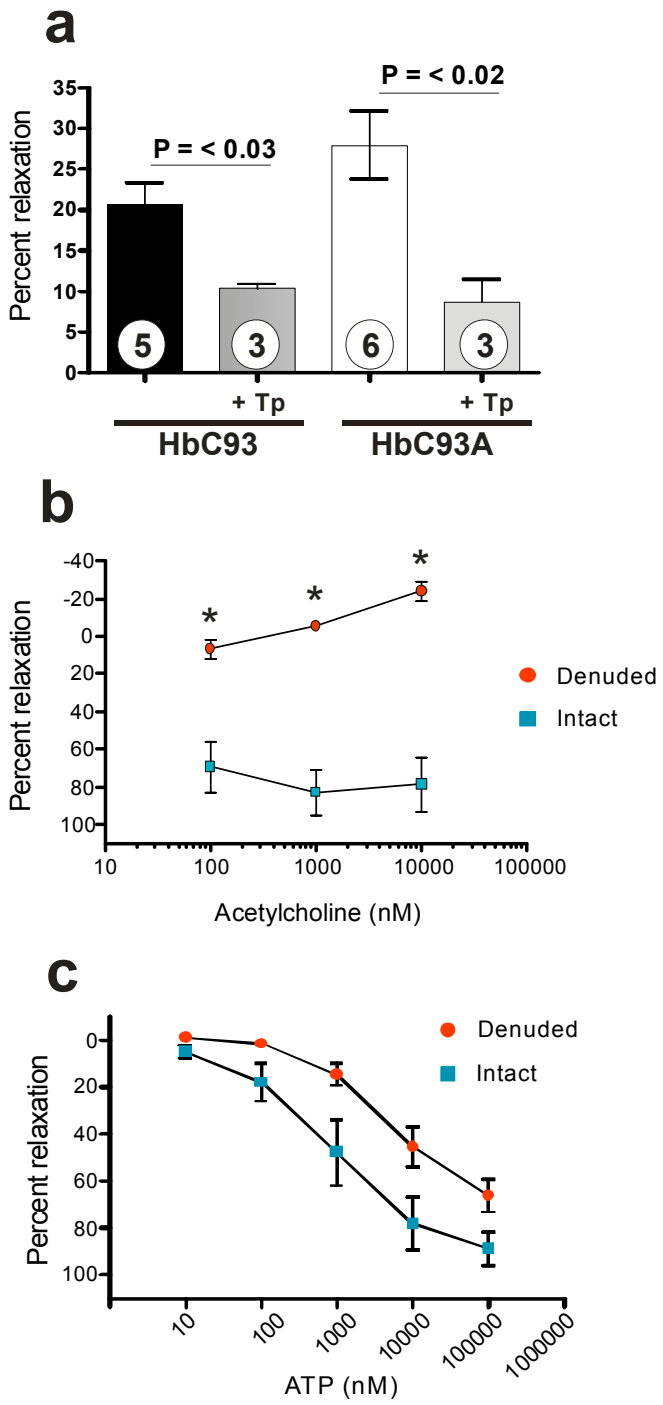

Supplementary Figure 7: Suppl Fig 7A demonstrates that both HbC93 and HbC93A RBCs dilate denuded rabbit pulmonary arteries to similar extents at low oxygen tensions (Suppl Fig 7B shows control experiments demonstrating adequate denudation, indicated by the loss of acetylcholine induced dilation; isolated rabbit pulmonary arteries were maintained intact or denuded by gentle rubbing of the lumen using a toothpick). Initially,

these data appear to suggest that ATP release is not involved in hypoxic dilation. However, ATP metabolism in the vascular compartment is complex and is mediated by multiple, poorly characterized enzymes (e.g. ecto-ATPases). The activities of these enzymes can result in the formation of secondary products including adenosine, which is an endothelium independent vasodilator. Therefore, we hypothesized that the formation of adenosine accounts for data shown in suppl Fig 7A. Consistent with this hypothesis, ATP itself still dilated denuded vessels albeit with a lower potency (Suppl Fig 7C) and the non-selective adenosine receptor antagonist, theophylline (Tp, 100μM), significantly inhibited both HbC93 and HbC93A hypoxic RBC dependent dilation of denuded vessels (Suppl Fig 7A). For Panel A: data shown are mean ± SEM, with n-values indicated in respective bars and P-values shown as calculated by unpaired t-test. For Panel B: data shown are mean ± SEM, n=3. *P = < 0.001 by 2-way ANOVA with repeated measures and Bonferroni post-test. All experiments were performed at 0% O_2.

Supplementary Material References

1. Wu, L.C. et al. Correction of sickle cell disease by homologous recombination in embryonic stem cells. *Blood* 108, 1183-8 (2006).
2. Kevil, C.G. et al. Regulation of endothelial glutathione by ICAM-1: implications for inflammation. *Faseb J* 18, 1321-3 (2004).
3. Patel, R.P. et al. Biochemical characterization of human S-nitrosohemoglobin. Effects on oxygen binding and transnitrosation. *J Biol Chem* 274, 15487-92 (1999).
4. Crawford, J.H. et al. Hypoxia, red blood cells, and nitrite regulate NO-dependent hypoxic vasodilation. *Blood* 107, 566-74 (2006).
5. Lang, J.D., Jr. et al. Inhaled NO accelerates restoration of liver function in adults following orthotopic liver transplantation. *J Clin Invest* 117, 2583-91 (2007).
6. Renfrow, M.B. et al. Analysis of O-glycan heterogeneity in IgA1 myeloma proteins by Fourier transform ion cyclotron resonance mass spectrometry: implications for IgA nephropathy. *Anal Bioanal Chem* 389, 1397-407 (2007).
7. Salazar Vazquez, B.Y., Cabrales, P., Tsai, A.G., Johnson, P.C. & Intaglietta, M. Lowering of blood pressure by increasing hematocrit with non nitric oxide scavenging red blood cells. *Am J Respir Cell Mol Biol* 38, 135-42 (2008).
8. Ellsworth, M.L., Forrester, T., Ellis, C.G. & Dietrich, H.H. The erythrocyte as a regulator of vascular tone. *Am J Physiol* 269, H2155-61 (1995).
9. Sprague, R.S., Ellsworth, M.L., Stephenson, A.H. & Lonigro, A.J. ATP: the red blood cell link to NO and local control of the pulmonary circulation. *Am J Physiol* 271, H2717-22 (1996).

10. Ellsworth, M.L. Red blood cell-derived ATP as a regulator of skeletal muscle perfusion. *Med Sci Sports Exerc* 36, 35-41 (2004).
11. Ellsworth, M.L. The red blood cell as an oxygen sensor: what is the evidence? *Acta Physiol Scand* 168, 551-9 (2000).
12. Gonzalez-Alonso, J., Olsen, D.B. & Saltin, B. Erythrocyte and the regulation of human skeletal muscle blood flow and oxygen delivery: role of circulating ATP. *Circ Res* 91, 1046-55 (2002).
13. Sprague, R. et al. Expression of the heterotrimeric G protein Gi and ATP release are impaired in erythrocytes of humans with diabetes mellitus. *Adv Exp Med Biol* 588, 207-16 (2006).
14. Nagababu, E., Ramasamy, S., Abernethy, D.R. & Rifkind, J.M. Active nitric oxide produced in the red cell under hypoxic conditions by deoxyhemoglobin-mediated nitrite reduction. *J Biol Chem* 278, 46349-56 (2003).
15. Cosby, K. et al. Nitrite reduction to nitric oxide by deoxyhemoglobin vasodilates the human circulation. *Nat Med* 9, 1498-505 (2003).
16. Huang, Z. et al. Enzymatic function of hemoglobin as a nitrite reductase that produces NO under allosteric control. *J Clin Invest* 115, 2099-107 (2005).
17. Basu, S. et al. Catalytic generation of N2O3 by the concerted nitrite reductase and anhydrase activity of hemoglobin. *Nat Chem Biol* 3, 785-94 (2007).
18. Angelo, M., Singel, D.J. & Stamler, J.S. An S-nitrosothiol (SNO) synthase function of hemoglobin that utilizes nitrite as a substrate. *Proc Natl Acad Sci U S A* 103, 8366-71 (2006).
19. Dalsgaard, T., Simonsen, U. & Fago, A. Nitrite-dependent vasodilation is facilitated by hypoxia and is independent of known NO-generating nitrite reductase activities. *Am J Physiol Heart Circ Physiol* 292, H3072-8 (2007).
20. Gladwin, M.T. et al. Nitrite as a vascular endocrine nitric oxide reservoir that contributes to hypoxic signaling, cytoprotection, and vasodilation. *Am J Physiol Heart Circ Physiol* 291, H2026-35 (2006).
21. Isbell, T.S., Gladwin, M.T. & Patel, R.P. Hemoglobin oxygen fractional saturation regulates nitrite-dependent vasodilation of aortic ring bioassays. *Am J Physiol Heart Circ Physiol* 293, H2565-72 (2007).
22. Kim-Shapiro, D.B., Schechter, A.N. & Gladwin, M.T. Unraveling the reactions of nitric oxide, nitrite, and hemoglobin in physiology and therapeutics. *Arterioscler Thromb Vasc Biol* 26, 697-705 (2006).
23. Luchsinger, B.P. et al. Assessments of the chemistry and vasodilatory activity of nitrite with hemoglobin under physiologically relevant conditions. *J Inorg Biochem* 99, 912-21 (2005).
24. Maher, A.R. et al. Hypoxic modulation of exogenous nitrite-induced vasodilation in humans. *Circulation* 117, 670-7 (2008).
25. Modin, A. et al. Nitrite-derived nitric oxide: a possible mediator of 'acidic-metabolic' vasodilation. *Acta Physiol Scand* 171, 9-16 (2001).
26. Rifkind, J.M. et al. Nitrite infusion increases cerebral blood flow and decreases mean arterial blood pressure in rats: a role for red cell NO. *Nitric Oxide* 16, 448-56 (2007).
27. Rogers, S.C. et al. NO metabolite flux across the human coronary circulation. *Cardiovasc Res* 75, 434-41 (2007).

28. Dejam, A. et al. Nitrite infusion in humans and nonhuman primates: endocrine effects, pharmacokinetics, and tolerance formation. *Circulation* 116, 1821-31 (2007).
29. Jia, L., Bonaventura, C., Bonaventura, J. & Stamler, J.S. S-nitrosohaemoglobin: a dynamic activity of blood involved in vascular control. *Nature* 380, 221-6 (1996).
30. Gaston, B., Singel, D., Doctor, A. & Stamler, J.S. S-nitrosothiol signaling in respiratory biology. *Am J Respir Crit Care Med* 173, 1186-93 (2006).
31. Gow, A.J. & Stamler, J.S. Reactions between nitric oxide and haemoglobin under physiological conditions. *Nature* 391, 169-73 (1998).
32. McMahon, T.J. et al. Nitric oxide in the human respiratory cycle. *Nat Med* 8, 711-7 (2002).
33. Pawloski, J.R., Hess, D.T. & Stamler, J.S. Export by red blood cells of nitric oxide bioactivity. *Nature* 409, 622-6 (2001).
34. Singel, D.J. & Stamler, J.S. Chemical physiology of blood flow regulation by red blood cells: the role of nitric oxide and S-nitrosohemoglobin. *Annu Rev Physiol* 67, 99-145 (2005).
35. Stamler, J.S. et al. Blood flow regulation by S-nitrosohemoglobin in the physiological oxygen gradient. *Science* 276, 2034-7 (1997).
36. Wolzt, M. et al. Biochemical characterization of S-nitrosohemoglobin. Mechanisms underlying synthesis, no release, and biological activity. *J Biol Chem* 274, 28983-90 (1999).
37. Zhang, Y. & Hogg, N. S-nitrosohemoglobin: a biochemical perspective. *Free Radic Biol Med* 36, 947-58 (2004).
38. Crawford, J.H., White, C.R. & Patel, R.P. Vasoactivity of S-nitrosohemoglobin: role of oxygen, heme, and NO oxidation states. *Blood* 101, 4408-15 (2003).
39. Giustarini, D., Milzani, A., Colombo, R., Dalle-Donne, I. & Rossi, R. Nitric oxide, S-nitrosothiols and hemoglobin: is methodology the key? *Trends Pharmacol Sci* 25, 311-6 (2004).
40. Gladwin, M.T. et al. Role of circulating nitrite and S-nitrosohemoglobin in the regulation of regional blood flow in humans. *Proc Natl Acad Sci U S A* 97, 11482-7 (2000).
41. Rassaf, T. et al. NO adducts in mammalian red blood cells: too much or too little? *Nat Med* 9, 481-2; author reply 482-3 (2003).
42. Huang, K., Azarov, I., Basu, S., Huang, J. & Kim-Shapiro, D.B. lack of Allosterically controlled intramolecular transfer of nitric oxide from the heme to cysteine in the beta subunit of hemoglobin. *Blood* 107, 2602-2604 (2006).
43. Joshi, M.S. et al. Nitric oxide is consumed, rather than conserved, by reaction with oxyhemoglobin under physiological conditions. *Proc Natl Acad Sci U S A* 99, 10341-6 (2002).
44. Xu, X. et al. Measurements of nitric oxide on the heme iron and beta-93 thiol of human hemoglobin during cycles of oxygenation and deoxygenation. *Proc Natl Acad Sci U S A* 100, 11303-8 (2003).
45. Fago, A., Crumbliss, A.L., Peterson, J., Pearce, L.L. & Bonaventura, C. The case of the missing NO-hemoglobin: spectral changes suggestive of heme redox reactions reflect changes in NO-heme geometry. *Proc Natl Acad Sci U S A* 100, 12087-92 (2003).

46. Kleinbongard, P. et al. Red blood cells express a functional endothelial nitric oxide synthase. *Blood* 107, 2943-51 (2006).
47. Hanna, J. et al. Treatment of sickle cell anemia mouse model with iPS cells generated from autologous skin. *Science* 318, 1920-3 (2007).
48. Carlson, S.H. & Wyss, J.M. Long-term telemetric recording of arterial pressure and heart rate in mice fed basal and high NaCl diets. *Hypertension* 35, E1-5 (2000).
49. Heximer, S.P. et al. Hypertension and prolonged vasoconstrictor signaling in RGS2-deficient mice. *J Clin Invest* 111, 445-52 (2003).